Water Resources Division
520 N. Park Ave, Suite 221
Tucson, AZ 85719
smwiele@usgs.gov
(520) 670-6671 277

February 26, 2004

MEMORANDUM

TO: Ted Melis, Physical Resources Program Manager, Grand Canyon Monitoring and Research Center

FROM: Stephen Wiele, Paul Grams, Josh Korman, Jack Schmidt, and Peter Wilcock

RE: Second year progress report on the Grand Canyon Modeling project

Over the past year, progress was made on development and application of the 1d and 2d models, development of methods to ease application of the models by other users, methods of general application of model results, and understanding and formulation of algorithms representing near-bed sand concentration over a rough boundary, a crucial component of the sand transport algorithms. In addition, valuable data were collected on a river trip in July, 2003 and a project meeting was held in Flagstaff in September, 2003. Seven presentations related to this project were made by project members (Appendix 1).

2d model

The following reaches were selected for modeling during the September, 2002 river trip: Cathedral, 22-mile, 30-mile, Silver Grotto, Eminence, 55-mile, 60-mile, 65-mile, and Palisades. Bathymetry for Cathedral, 22-mile, and 30-mile has been obtained from NAU. Eminence bathymetry was obtained from the GCMRC web site. Palisades and 65-mile are available from previous projects. The model has been applied to the reaches for which bathymetry is available with the exception of Cathedral. Silver Grotto, 55-mile, and 60-mile have been surveyed by the GCMRC, but are not yet available. Results from the 2d modeling examined so far indicate that accumulation rates at each site may be characterized with reasonable accuracy with a simple exponential function of the form $dv/dt = ae^{(-bv)}$ where v is volume, t is time, a and b are constants determined from the modeling results for each reach, and e is the natural log base.

Methods for applying the 2d model and viewing the results have been developed that are a combination of command-line operation (which facilitates running the model in batch mode) and visualization provided by Tecplot, a proprietary fluid mechanics graphics package originally developed by NASA and distributed by Amtec. This combination provides the most convenient and efficient method of using the 2d model. Input to the model is controlled by standard input files that contain sediment input to the reach as a

function of time, stage, and discharge. The model is run in batch mode with a DOS BAT file that changes the input for each case by renaming directories to the default names and then launching the model. A method has been developed for viewing 2d model results and developing animations using Tecplot. The model writes out files containing flow and sediment transport fields as well as updated bathymetry at 1-hour simulated time intervals. These files are in a format that can be read by Tecplot. Macro files have been written that are read by Tecplot for the generation of animations. Model grids for seven reaches from a previous project (Korman and Wiele, Modeling Effects of Discharge on Habitat Quality and Dispersal of Juvenile Humpback Chub (*Gila cypha*) in the Colorado River, Grand Canyon) have already been delivered to the GCMRC and the grids used in this project will be delivered at the end of this project. A method of generating grids for new reaches using Tecplot and two utility programs have been developed; a description of that method and the utility programs will be delivered to the GCMRC as a product of this project.

1d model

Reach geometry
Cross sections between river mile -15 and 88 have been received from the GCMRC (Mike Breedlove, written communication) and edited for cross sections extending up side canyons and near-water surface errors. The 97k river stage at each cross section extracted by the GCMRC from BOR GIS coverage is anticipated soon and will be used in generating reach averaged cross sections to scale channel width above the 8k water surface. Programs have been completed for computing reach-averaged channel shape for discrete river miles for both the above 8k cfs water surface represented in the GIS coverage, and the below 8k water surface, for which the Wilson cross sections will be used. A general stage-normalized curve (Wiele and Torizzo, 2003), along with the difference between the reach-averaged 97k and 8k water surface elevations will be used to calculate the hydraulic geometry

At the September project meeting, the following river miles were chosen as the sub reaches in the 1d model:

-15 – 0
0 – 11.3
11.3 – 25.2
25.2 – 41.9
41.9 – 60.3
60.3 – 65.9
65.9 – 77
77 – 87

These reaches are based on the work of Jack Schmidt, who determined reaches of similar morphology based on bedrock type and are similar to the Melis designations based on fan characteristics.

Extrapolation of 2d results used in the 1d model

One of the essential components of the one-dimensional sand routing model is a representation of the sand storage potential in each of the geomorphic reaches between Glen Canyon Dam and the Grand Canyon Gage. Although eddies are not the only storage locations for fine-grained sediment, they are the primary sink for channel-side sand in most reaches downstream from Lees Ferry. It is therefore necessary to develop some means of characterizing the number and size of eddies in each model reach. The Geomorphology group at USU has characterized a subset of eddies by studying aerial photos and noting the extent of sand near the eddy shown in the photos. The maximum extent of the depositional area associated with an eddy is called the MPAEB. At our September meeting, we discussed two approaches for extending these results to the entire study area. One approach is to identify each eddy and estimate its boundary. Identification of the MPAEBs at new sites would rely on the experience and judgment of Jack Schmidt gained from extensive examination of maps and aerial photos during the earlier work. USU has implemented another approach in which the eddy size and distribution is modeled statistically. This method was developed by Dave Galbraith, Paul Grams, and Jack Schmidt and is described in the paragraphs below.

We have used the USU GIS map database and the longitudinal bed profile to develop statistical models in an initial attempt to characterize eddy size and distribution. These models use eddy size and frequency as dependent variables and 9 independent variables, based on local and reach geomorphic characteristics.

The independent variables include four measures of debris fan characteristics, three measures of bed elevation, and two measures of local channel morphology. The debris fan metrics were (1) fan area, (2) fan frequency, (3) channel expansion factor, and (4) fan-shape factor. Fan area and frequency were determined from the USU GIS database. The channel-expansion factor was calculated from the GIS maps as the ratio of one-half the channel width at the expansion to one-half the channel width of the upstream constriction. The fan-shape factor is width divided by length. All of these metrics were normalized for each sample unit. The bed elevation metrics were (1) average variance from the linear-regressed mean thalweg elevation, (2) the 90^{th} percentile water depth, and (3) the water-surface slope. The metrics of channel morphology were (1) mean-channel width, and (2) valley confinement ratio. The confinement ratio was calculated as the ratio of alluvial valley width to channel width.

In order to determine the best spatial scale for averaging, we considered six sample unit definitions. These consisted of 1-mi, 2-mi, and 4-mi segments. Each of these segments was tested as a lumped sample and a side-specific, or split sample. In the split samples, the statistical models were executed separately for each side of the river.

All data were imported into the SAS for statistical analysis and 24 separate statistical models were run. An adjusted R^2 selection criteria indicated that the best sample unit was the 4-mi side-specific segment. The significance of each independent variable was assessed using the adjusted R^2 selection method, the Akaike Information Criterion, and Type I partial correlation. The variance in bed elevation and debris fan frequency were

the best predictors of eddy frequency. The valley confinement ratio and the debris fan area were the best predictors of eddy size. Adjusted R^2 were 0.61 and 0.84 for the eddy frequency and eddy size models, respectively.

The GIS data used in these analyses are currently available only for the reaches included in the USU GIS database, which covers a total of about 34 mi of the 87 mi between Lees Ferry and the Grand Canyon Gage. The Bureau of Reclamation longitudinal bed profile is available for the entire reach. In order to apply this analysis to the entire study area, we have conducted additional mapping that was guided by this analysis. To enable calculation of the confinement ratio, one the most significant independent variables, at the scale of 3- to 4-mi segments, we have digitized the alluvial valley boundary for the entire study area. The next step in this project is to incorporate these new data in the statistical models.

1d GUI

Tributary sediment input algorithms have been integrated into the latest version of the Colorado River Flow, Stage, and Sediment Graphical User Interface (CRFSSGUI). The model now predicts the input of silts and clays from the Paria River and sand from both the Paria and LCR rivers based on observed discharges and rating curves provided by D. Topping (USGS, Grand Canyon Monitoring and Research Center, unpublished data). Total silt/clay and sand input is computed as the product of water discharge and the sediment discharge predicted by the rating curves. The interface allows the user to determine the total sediment load over specific periods or examine the temporal trend in inputs. The interface also has the ability to download provisional water discharge data from the USGS web site into a format that can be read by CRFSSGUI. These data can then be used to predict sediment inputs and can also be included in the computation of temporal and spatial patterns in discharge predicted by the unsteady flow component of the interface.

The most recent version of the downstream sediment routing algorithm being developed as part of this project has been incorporated into CRFSSGUI. The interface allows the user to select a mainstem discharge file to drive model predictions. Other boundary conditions are currently hardwired in the computer code but will be available for review and editing in the final version of the model. The interface allows the user to display temporal and spatial patterns in sediment concentration and sediment discharge for the grain sizes that are modeled in the sediment-routing algorithm.

Additional technical issues in the 1d model

Some technical issues with the 1d sand model were also addressed. A constrained instability in the sand transport that appeared intermittently was traced to the sand transport turning on and off as the sand coverage declined. Switching to an implicit solution in the sediment continuity equation at a critical sand thickness seems to have eliminated this problem, yielding a more realistic, smoother solution and increasing the time step (which shortens runtimes). Different ways of formulating the suspended sediment algorithm were compared, and the potential stability advantages available by including advection in the solution appeared to be small. The semi-analytical solution involving a Rouse profile allows for a coarser vertical grid than can be used with a fully

numerical solution, reduces the possibility of pathological numerical behavior, and with the fix described above, does not appear to generate any stability problems.

Initial model applications

As a test of the 1d model's ability to handle time periods on the order of months and as an initial test of the model's sand transport predictions, the 1d model was applied to the period from 9/1/1995 to 6/1/1996 and from 10/1/99 to 9/12/00. The experimental release of 1996 occurred during the earlier time period, from March 26 to April 2, and the Low Steady Summer Flows, with spike flows of about 900 cms, occurred during the second time period. The discharge record at Lees Ferry was used to set the upstream boundary condition for the water discharge. A slug of sediment with a d50 of 0.13 mm at the mouth of the Paria River was specified early in the simulations (Fig. 1).

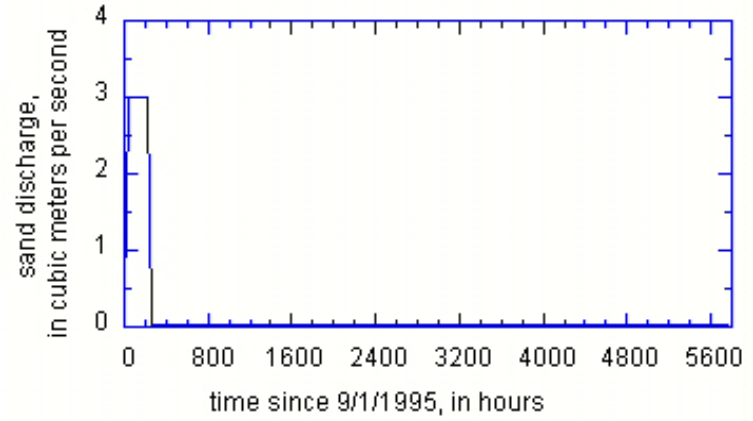

Figure 1. Sand discharge into the main stem specified at the upstream boundary in the 1d model application. A similar sand input was specified for the model application to the LSSF flows, but started on 10/1/99.

It was anticipated that the bulk of the sand input specified at the beginning of the simulation would be routed through prior to the experimental high flows and that the transport rates would asymptotically approach a more gently declining ambient transport that would be a reasonable approximation of the transport rates prior to a high flow. The simulations of flow and sand transport took about 9 hours on a 2.4 GHz computer with a Windows2000 operating system. At the Grand Canyon gage, 87 miles downstream, the model predicts a sand concentration that varies with the fluctuating discharge and with an overall declining trend (Fig. 2 and 3).

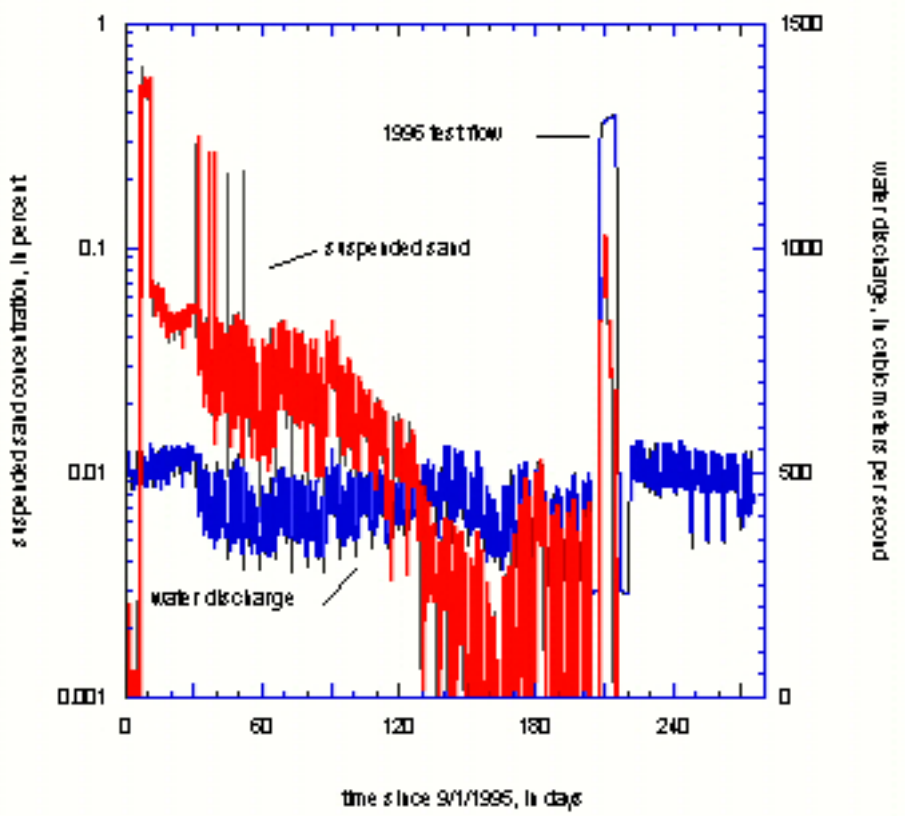

Figure 2. Suspended sand concentration (red) and water discharge (blue) predicted by the 1d model at the Grand Canyon gage prior to and during the 1996 experimental release.

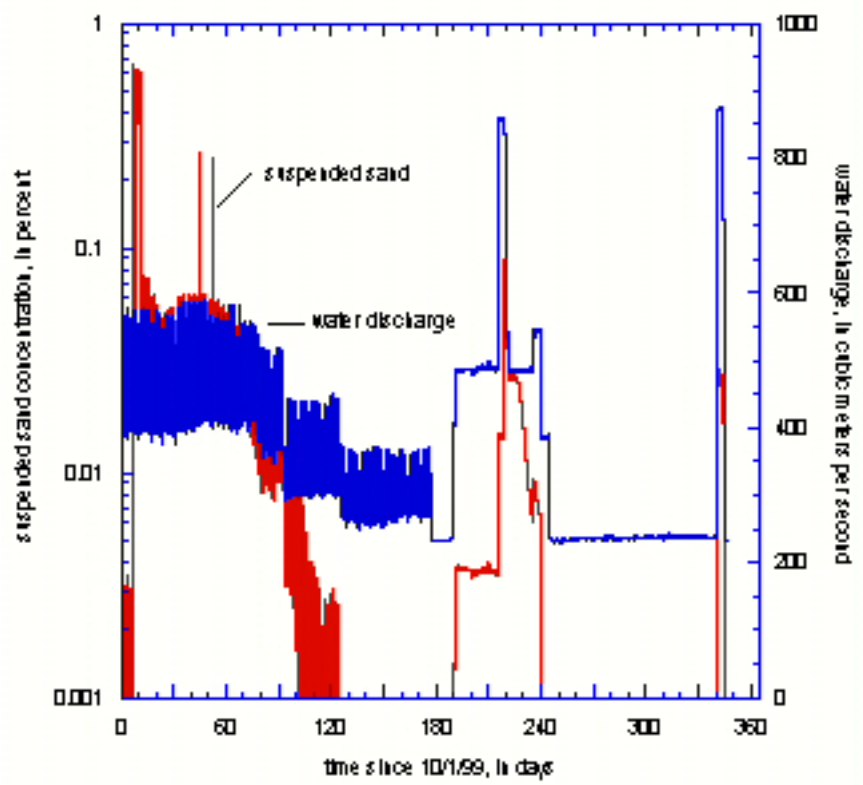

Figure 3. Suspended sand concentration (red) and water discharge (blue) predicted by the 1d model at the Grand Canyon gage during and prior to the spike flows during the LSSF experiment.

Only one sand input was specified, and neither the model nor the sand input was adjusted in any way to achieve a desired result. Despite the approximate initial condition and algorithm for near-bed sand concentration currently in the model, the model predictions of peak sand concentration during the 1996 experimental flow and the two spike flows during the LSSF experiment are reasonably close to the measured peak values of 0.11 (Topping and others, 1999), 0.101, and 0.05 percent, respectively (Figs. 4, 5, and 6).

The model shows a delay between the peak sand concentration and the initiation of the peak flow, whereas measurements show peak sand concentration at the Grand Canyon gage tends to coincide with the initial rise of the higher discharge. This delay will probably be affected by more accurate initial conditions, addition of side-channel sources and sinks, more accurate representation of bed characteristics, and the more accurate near-bed sand boundary condition currently under development as part of this project.

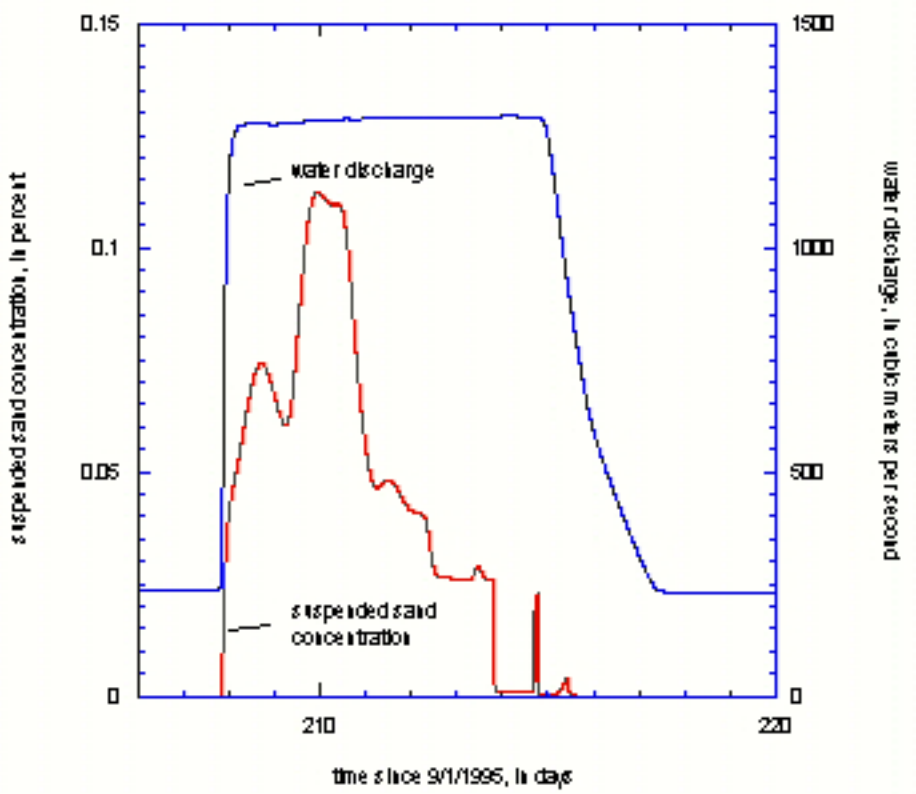

Figure 4. Suspended sand concentration (red) and water discharge (blue) predicted by the 1d model at the Grand Canyon gage during the 1996 experimental release. The peak sand concentration measured at the Grand Canyon gage during the experimental release was 0.11 percent (Topping and others, 1999).

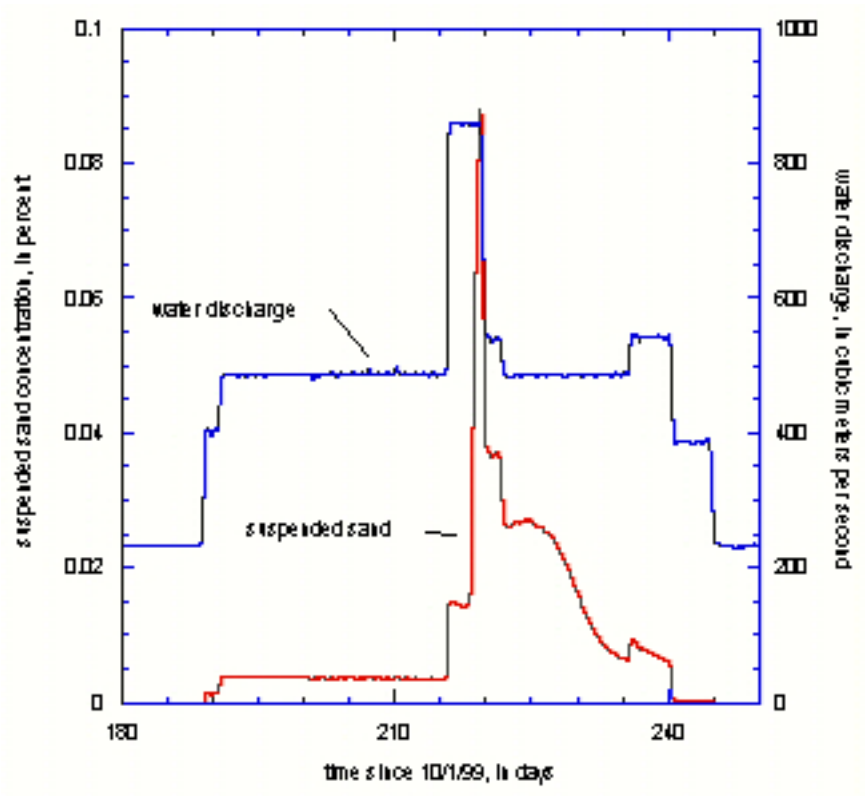

Figure 5. Suspended sand concentration (red) and water discharge (blue) predicted by the 1d model at the Grand Canyon gage during the March 2000 LSSF spike flow. The peak sand concentration measured at the Grand Canyon gage during the March 2000 LSSF was 0.10 percent.

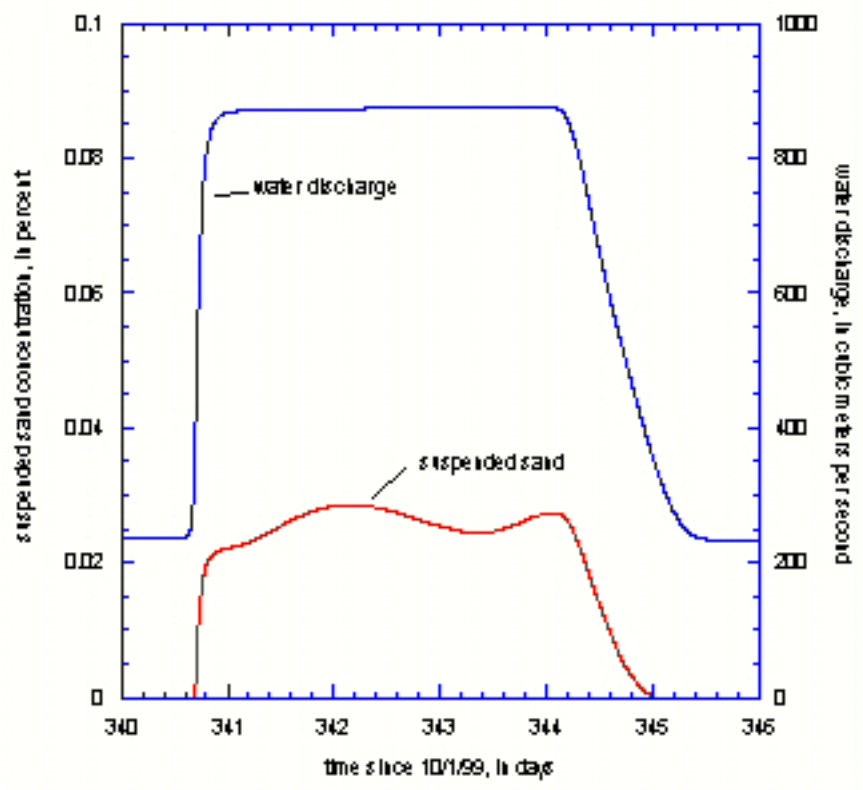

Figure 6. Suspended sand concentration (red) and water discharge (blue) predicted by the 1d model at the Grand Canyon gage during the September 2000 LSSF spike flow. The peak sand concentration measured at the Grand Canyon gage during the March 2000 LSSF was 0.05 percent.

Characterization of Bed Roughness

Video of the channel bottom was taken with the GCMRC rig during a river trip in July 2003. The video shows the size of clasts, sand deposits, and sand in transport near the bed. Video was taken at 231 locations at 104 cross sections between Lees Ferry and Phantom Ranch (Fig. 7). Sand samples were taken at 13 locations, but grain size analyses have not yet been reported by the GCMRC.

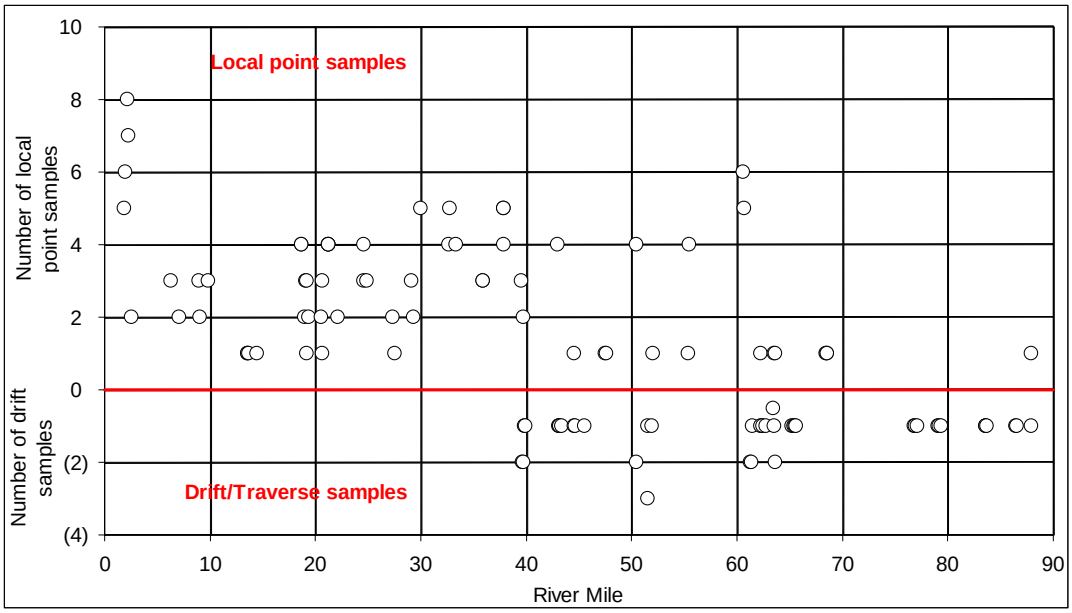

Figure 7. Locations of video samples.

Each video sample consists of digital video imagery covering the bed for a short distance (point sample) or traversing across most of the channel (transect sample). The camera was suspended a short distance above the bed such that the parallel lasers positioned 10 cm apart are visible in the center of the image. These lasers provide a scale that can be used to estimate grain sizes of sediment on the bed. However, because the camera angle was oblique, not vertical, the lasers provide a scale in one dimension only. If this camera is to be used extensively, a third laser would improve our ability to resolve the scale in two dimensions.

These data will be analyzed at USU to characterize the bed for each of the transect locations. We will estimate a grain-size distribution near the channel center and qualitatively describe the center and sides of each transect including an estimate of sand cover. We will also attempt to determine the degree to which the transect locations are representative of their respective reaches by examination of maps of channel-bottom textures Roberto Anima (USGS-GD) interpreted from his side-scan sonar images.

The grain-size distribution will be estimated by measuring individual grains in the video images. This will be done using software developed by Ecometric Research for this purpose (Bed Video Image System, BVIS). Digital video files, once transferred from tape to computer using commercially available digital video editing software, can be loaded into BVIS to capture a single still image from the video segments for each measurement location. The user then identifies the laser points on the still image so that the scale of the image can be determined. A transect that intersects the laser points is automatically drawn across the entire width of the image and divided into a user-determined number of equal widths. The b-axis of each clast located at the intersection of the transect and width boundaries is measured by the user and automatically recorded by the software. By measuring grains along an axis where the scale is known, the width of the grains in pixels can be translated into an absolute unit of measurement (mm).

Software development has been completed by Ecometric Research and processing of the bed video imagery is underway at USU. BVIS is available for download at http://www.mountainsoft.net. Costs of software development were shared between this cooperative agreement and 98fc4022580. The work will result in bed material characterization for each reach, expressed as a D90, and the proportion of the reach for which that number is reasonably representative.

Laboratory Experiments to Support the Development of a Sand Routing Model

The objectives of this research are to test, through laboratory experiments, two separate but related components of the Grand Canyon sand routing model. These components are (1) a functional relation for the rate of sand entrainment from the bed, dependent on flow and bed conditions, and (2) the sediment mass balance algorithm for routing transported sediment. Laboratory experiments are being conducted because sand entrainment models have not been tested for transport over an immobile bed with a roughness much larger than that of the transported material.

The proposed research consists of two separate sets of laboratory flume experiments. The first set (completed in 2002) was designed to test sand entrainment under uniform transport conditions over a coarse bed. Data from these experiments are used to evaluate the application of existing entrainment models and to construct a preliminary entrainment model for large-bed roughness. The experimental arrangement and preliminary results from these experiments were described in our 2003 progress report. In this report, we present our more complete analysis of flow conditions for the flume experiments and our proposed entrainment model. The second set of experiments is designed to test the application of the sand entrainment model to routing sediment in nonuniform transport conditions. The rational and design for those experiments is presented below. Together, these experiments evaluate the effect of sand-bed elevation among large bed roughness on sand entrainment, provide data that will be used to modify existing models or develop a new model, and test the model in uniform and nonuniform transport conditions.

Measurement of Instantaneous Velocity

The 18 experimental runs were conducted at eight different flow rates. For each flow rate, profiles of instantaneous velocity were measured at three locations in the vicinity of the sediment sampling station (Figure 8). Each profile consists of seven measurements made at elevations of 0.5, 1, 2, 5, 10, 20, and 30 cm above the tops of the roughness elements. Velocity measurements in downstream, cross-stream, and vertical directions were collected using an acoustic Doppler velocimeter (ADV) sampling at a rate of 25 hz for approximately one minute. All velocity measurements were collected during clear flow conditions when there was no sediment in suspension or on the bed.

Before the ADV data could be analyzed for turbulence characteristics, it was necessary to process the raw data to remove spikes and correct for instrument misalignment. Spikes in ADV data are caused by aliasing of the Doppler signal that may occur when the phase shift between the outgoing and incoming pulse lie outside the range between –180° and +180° causing ambiguity in the signal. This situation can occur when the velocity

exceeds the set velocity range or as a result of signal contamination from previous pulses reflected from complex bottom geometries. Because measured velocities never approached the limit of the sampling range (2.50 m/s), all of the spikes in the ADV records are likely due to the bottom geometry. These spikes were removed by a phase-space threshold despiking method described by Goring and Nikora (2002) and implemented in the WinADV software by Wahl (2000, 2003). Goring and Nikora (2002) found this method the most satisfactory in detecting anomalous spikes while leaving intact true spikes due to turbulent fluctuations in the velocity. Spikes detected by this method were removed from the record and not replaced with interpolated or other values. Figure 9 shows an example of an ADV record before and after despiking.

Following despiking, it was also necessary to correct the data for probe misalignment. The velocity probe was mounted on the end of a steel point gage mounted over the flume. Although the point gage was mounted as securely as possible and positioned for proper probe orientation, drag on the point gage and probe once in the flow caused slight misalignment of the probe. This misalignment results in non-zero mean velocities in the cross-stream and vertical directions. The data were adjusted by rotating the coordinate axes to result in zero mean velocities in the vertical and cross-stream directions. Rotation angles were typically on the order of 3° to 5°.

Calculation of Reynolds Stresses

After processing the ADV records, mean velocities and turbulence statistics were calculated from the filtered and rotated data. The turbulent Reynolds stress τ_{zx} was calculated at each elevation in the flow as

$$\tau_{zx}(z) = -\rho\overline{(u'w')},$$

where z represents height above the bed, ρ is the fluid density, u and w are the streamwise and vertical components of velocity, taken positive in the downstream and upward directions, the overbar represents time-averaged quantities and the primes denote instantaneous deviations from the mean (i.e. $u' = u - \overline{u}$). The corresponding shear velocity u_* was calculated as

$$u_*(z) = \sqrt{\tau_{zx}/\rho}\ .$$

Velocity Profiles

Profiles of mean velocity were plotted and examined for each measurement station for each flow rate. For most of the flow rates, measurements were made only at the three stations described above. However, for one flow rate measurements were made at roughly 1 m intervals along the length of the flume. These data show the development of the rough flow profile and indicate that at distances of 8 to 11 m downstream from the flume headbox fully developed flow conditions existed (Figure 10). The development of the velocity profile is also shown by an examination of the velocity defect profile. The velocity defect is calculated as

$$\frac{(u_s - u)}{u_*}$$

where u_s is the surface velocity, taken as the measured velocity 30 cm above the hemisphere tops. Figure 11 shows the velocity defect profile measured 3.0 m downstream from the entrance and Figure 12 shows the average velocity defect profile for the sediment measurement station (10.6 m downstream from the entrance). At the upstream position the profile is much steeper and the upper part of the flow does follow a logarithmic velocity defect profile. At the downstream position the point velocities measured at 2 to 30 cm above the hemisphere tops fit the expected logarithmic velocity defect distribution quite well.

The three velocity profiles collected in the vicinity of the sediment sampling station were used to examine the vertical structure of the flow and the spatial variation of the flow near the sampling station. Figures 13 and 14 show all the measured profiles of velocity and shear velocity (as calculated from the local Reynolds stress) normalized by the mean velocity of the flow. These profiles indicate that there existed a well-mixed region of the flow in the first 2 cm above the tops of the roughness. Figures 15 and 16 show the profiles of velocity and shear velocity averaged among the flow rates and three measurement positions. The error bars show +/- one standard deviation. From 0.5 to 2 cm above the hemisphere tops, velocity increases slightly in a log-linear relationship. Between 2 cm and 30 cm above the roughness elements, velocity increases in a log-linear relationship.

The variation of u_*/u in the 0.5 to 2 cm range is not correlated with either the magnitude of the mean flow velocity or the measurement position, in fact the mean u_*/u for the three measurement positions is similar (Figure 17). It therefore appears that shear stress in the region above the hemisphere tops may be best represented as a simple function of mean flow velocity.

$$u_{*b} = 0.07U$$

where u_{*b} represents the near-bed shear velocity. Analysis of the residuals of the predicted estimates of u_{*b} as compared to the measured values of u_* at 0.5, 1.0 and 2.0 cm indicate a root-mean-square error of 0.01. The error is approximately the same among the different measurement positions and elevations.

Flow Non-Uniformity and Total Boundary Shear Stress

Non-uniform flow conditions at the flume entrance and exit caused measurable variations in depth at the upstream and downstream ends of the flume and smaller variations in the center region (Figure 18). To estimate the effect of this non-uniformity on our modeled bed stress u_{*b}, we calculated total boundary shear stress independently using the shallow-water equation and compared it with an estimate of total boundary shear stress based on our modeled bed stress. This approximation was accomplished using a flume sidewall correction procedure.

The non-uniform flow total boundary shear stress $\tau_0(N)$ was calculated using the shallow water equation

$$\tau_0(N) = \rho g R\left[S_0 - \frac{dh}{dx} - \frac{U}{g}\frac{du}{dx} \right]$$

where S_0 is the slope of the flume bed (0.0002). The hydraulic radius R and local velocity u were calculated from the measured depths. The section mean velocity U was calculated as the average of each two adjacent local velocities. The gradients in depth and velocity were determined by backward differences from each measurement position, starting with the second station downstream. This calculation yielded variations in τ_0 comparable to the variations in depth, with a region of constant $\tau_0(N)$ near the sediment sampling station.

The modeled total boundary shear stress $\tau_0(m)$ was estimated from the modeled near-bed stress using the flume sidewall correction procedure of Vanoni (1975) and modified by Chiew and Parker (1994). In the sidewall correction, the bed friction factor is calculated based on the friction factor for the total flow and that of the sidewall. The sidewall friction factor is estimated from a standard relation between friction factor and Reynolds number **R** for a hydraulically smooth surface, where $\mathbf{R} = 4Ur/\nu$, r is the hydraulic radius and ν is kinematic viscosity. The bed portion of the shear stress τ_b is then calculated from the bed friction factor. The total stress $\tau_0(m)$ is related to τ_b and the wall stress τ_w as

$$\tau_0(m)PL = \tau_b P_b L + \tau_w P_w L$$

where L is a length of bed in the streamwise direction and, for a rectangular flume, $P_b = b$ and $P_w = 2h$. The modeled bed stress is approximately 2.5 times the wall stress and 1.8 times the total stress (Figure 19).

Figure 20 shows $\tau_0(N)$ compared with $\tau_0(m)$ for the region in the vicinity of the suspended sediment sampling station where $\tau_0(N)$ shows the least downstream variation. Although there is considerable scatter in the boundary stress calculated from the shallow-water equation, that estimate of stress is generally consistent with the modeled stress across a broad range of flow velocities.

Relationship between bed shear stress and the stress acting on grains of sand

Laboratory and field data have frequently demonstrated that the rate of bed particle entrainment is proportional to the shear stress acting on those particles. The central difficulty lies in properly defining and characterizing the stress acting on grains available for transport. For a planar bed composed of uniform sediment, the stress acting on those particles may be adequately represented by the total boundary shear stress. However, it has long been recognized that for non-planar beds, the total bed shear stress includes stresses acting on the bed at multiple scales. For this reason, the total bed stress is often partitioned to include one component that act on large-scale bed roughness elements, such as dunes, and a second component that acts on small-scale roughness elements, such as the grains available for transport. The stress acting on the immobile bed roughness

elements is typically referred to as form drag and the stress acting on the sand grains as grain stress.

Stress partitioning is essentially a means of scaling the spatially averaged bed stress to estimate the spatially averaged grain stress. This spatially averaged grain stress is not the actual stress acting on individual grains and the relationship between the spatially averaged grain stress and the actual grain stress is poorly understood. In a bed composed of large roughness elements with finer particles in the interstices of those elements, the flow among those roughness elements is complex.

In an effort to characterize the form drag acting on the large roughness elements of our flume experiments, we used the procedure described by Wiberg and Smith (1991) and Nelson et al. (1991). We found that for our flow conditions and bed geometry this method was extremely sensitive to the choice of initial velocity profile and the choice of the turbulent length scale. We experimented with running the model a couple of different ways, and found, in general, that form drag is predicted to account for essentially all of the bed stress. This is really not surprising, given the entrainment environment among the roughness elements. Sand entrainment occurs in the wakes of the large grains, and as Nelson et al. (1995) demonstrated, particle entrainment in wakes is not always associated with turbulent events that contribute positively to bed shear stress. We have, therefore, chosen to keep the stress characterization simple and base the entrainment model on total bed stress.

Proposed Sand Entrainment Model

We identified in the 2002 flume experiments that it was possible to maintain a sand bed among large roughness elements only for a narrow range of flow and sediment feed conditions. Outside of this range, either all of the sediment would remain in suspension and no sand bed would form, or sediment would accumulate rapidly on the bed and migrate downstream as a coherent dune. Conditions with a stable sand bed ("target bed") were achieved for four sediment feed-discharge combinations (Figure 21). This narrow range suggests that for fine sediment transport over a coarse bed, there may exist a threshold combination of flow and sediment concentration capable of maintaining a sand-covered bed. Below this threshold, sand in particle interstices may be rapidly evacuated, presumably due to wakes shed by the roughness elements once flow separation occurs. The threshold range appears to be broader for coarser sand.

Our approach for implementing these observations is to apply correction functions to a standard entrainment model that predicts near-bed concentration for transport over a sand-covered bed. This function modifies the predicted near-bed concentration for a sand-covered bed $\hat{c}_a$ such that $c_a = F_s \phi \hat{c}_a$, where c_a is the near-bed concentration, F_s is the fraction of the bed area covered by sand, and ϕ is a function that accounts for the elevation of the sand bed among the roughness. F_s and ϕ may be treated independently or together. Figure 22 compares modeled near-bed concentrations compared with those observed in the flume runs. The observed concentrations have been adjusted to account for the proportion of the bed covered by sand, such that the plot is comparing measured

c_a/F_s with modeled $\hat{c}_a$, leaving out ϕ. For our flume experiments, both models over predict the observed concentrations and the Garcia and Parker model seems to fit the observations better than the Smith and McLean model. To find a function for ϕ, one might look at the relationship between ϕ as calculated from the experimental data and measurements of the sand bed elevation (Figure 23). This relationship shows wide scatter and does not suggest any straightforward relationship between ϕ and the sand-bed elevation. When there is less sand on the bed, by area, ϕ tends to be equal to or greater than unity, indicating that c_a is adequately predicted by $\hat{c}_a F_s$. This applies to the situation towards the lower end of the threshold for maintaining a sand-covered bed. When there is more sand on the bed, ϕ is between 0.3 and 0.6, with no significant trend as a function of sand-bed elevation. Figure 24 is a plot showing the combined effect of F_s and ϕ, calculated as $c_a/\hat{c}_a$ as a function of the fraction of the bed covered by sand. In the range of bed conditions treated in the flume runs, $F_s\phi$ varied between about 0.15 and 0.40, with no significant trend as a function of the amount of sand on the bed. This suggests that F_s and ϕ may be treated together as a constant within the range of partially-filled bed conditions. However, as the bed becomes completely filled with sand and the true sand-bed condition is approached, $F_s\phi$ must approach unity. Figure 24 also shows a possible function for $F_s\phi$, treating it as constant for most of the range of bed conditions, then increasing rapidly to unity between $F_s = 0.6$ and $F_s = 1.0$. This relation may be expressed as

$$F_s\phi = A + \frac{F_s^{\,k}}{B + \frac{F_s^{\,k}}{1-A}}$$

where A is the constant value of $F_s\phi$ that applies among the roughness elements, k determines the slope of the curve stepping up from A to unity, and B is a constant that forces the function to approach unity at $F_s = 1.0$. For the data shown in Figure 24, $k = 15$, $A = 0.26$, and $B = 0.01$. The modeled near-bed concentration is shown plotted against the observed near-bed concentration in Figure 25.

This discussion is provided as an example of how our entrainment model is taking shape. We have other factors to consider, such as the appropriate height for calculating the near-bed concentration. Our measured concentration profiles indicated that the concentration at 2 cm above the roughness elements provided a better anchor for a Rousean concentration profile than the 0.5 cm elevation. In the above discussion on the entrainment model, I used the concentrations measured at 0.5 cm, because those data provided a better match to the concentrations predicted by the entrainment models. We could bridge the gap between the 0.5 cm and 2 cm locations using an empirical relation based on our laboratory data, or reformulate the model based entirely on the 2 cm elevation.

Laboratory experiment figures

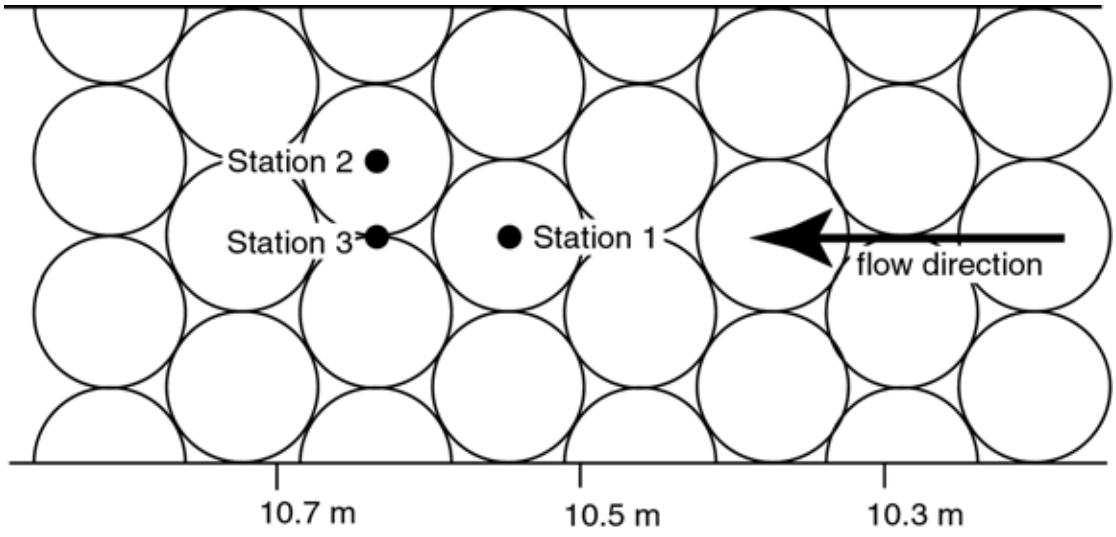

Figure 8. Sediment sampling stations.

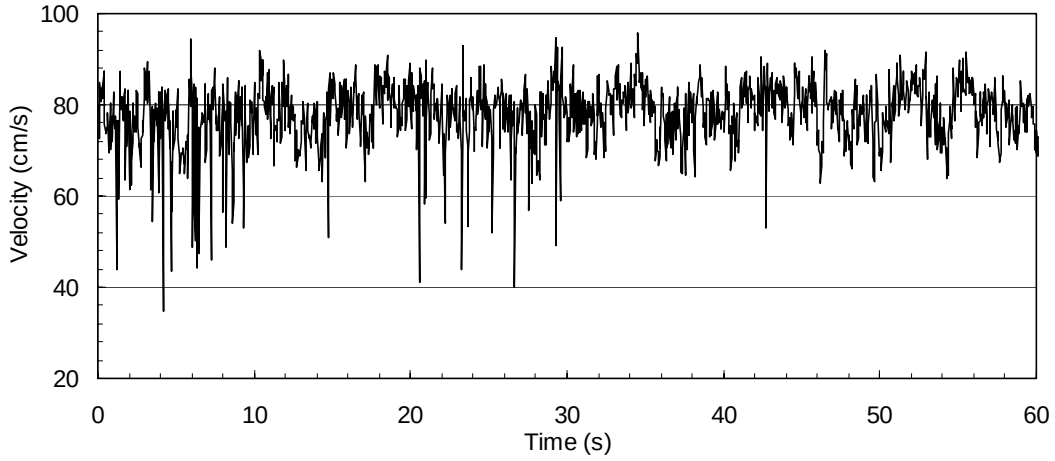

Figure 9A. Unfiltered ADV data.

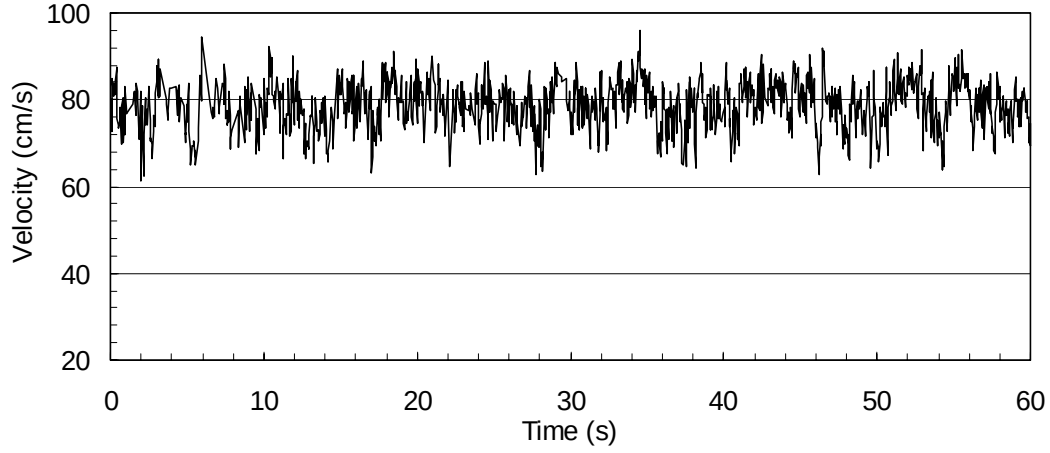

Figure 9B. Filtered ADV data.

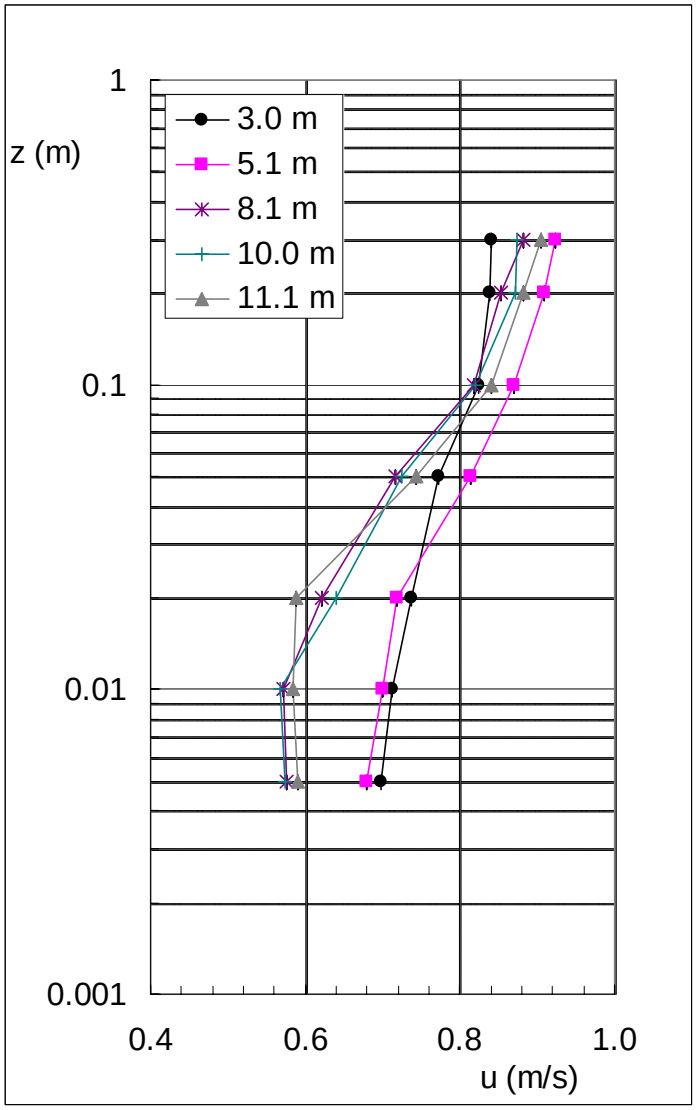

Figure 10. Development of velocity profile from flume entrance. Each profile is from the indicated distance downstream from the flume headbox.

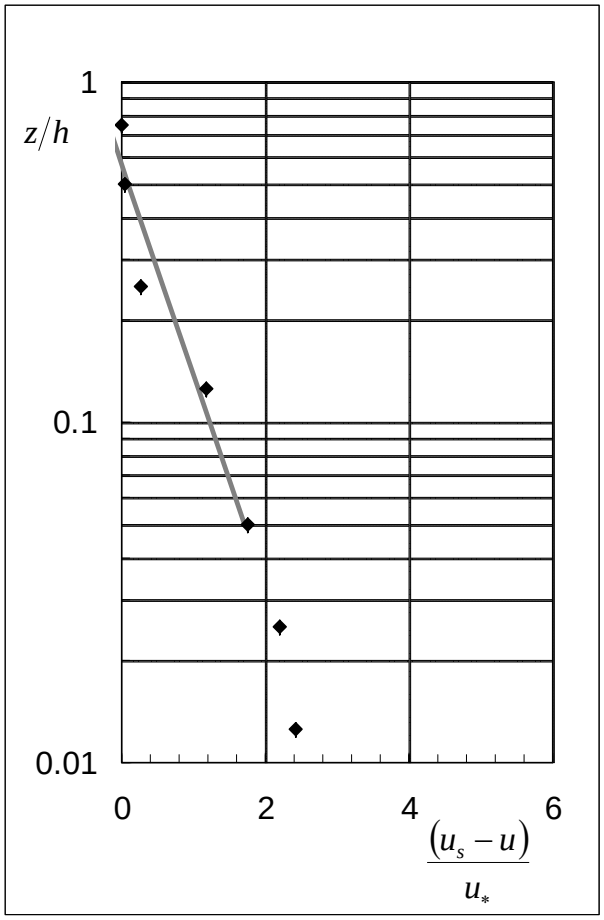

Figure 11. Velocity defect profile 3.0 m downstream from flume headbox.

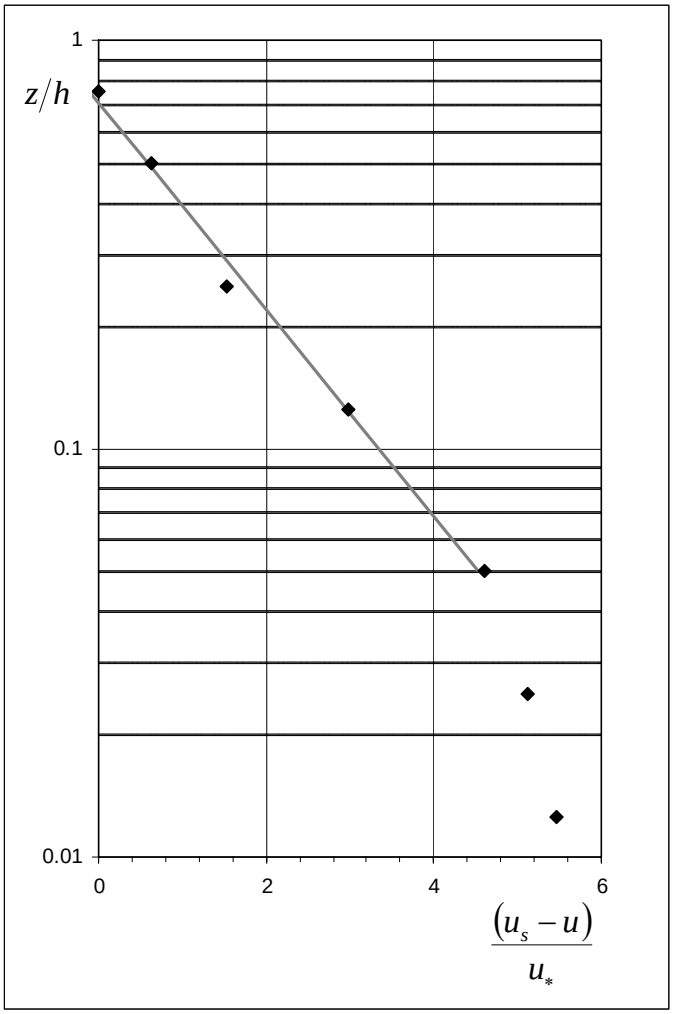

Figure 12. Velocity defect profile based on spatially averaged and flow averaged velocity measurements.

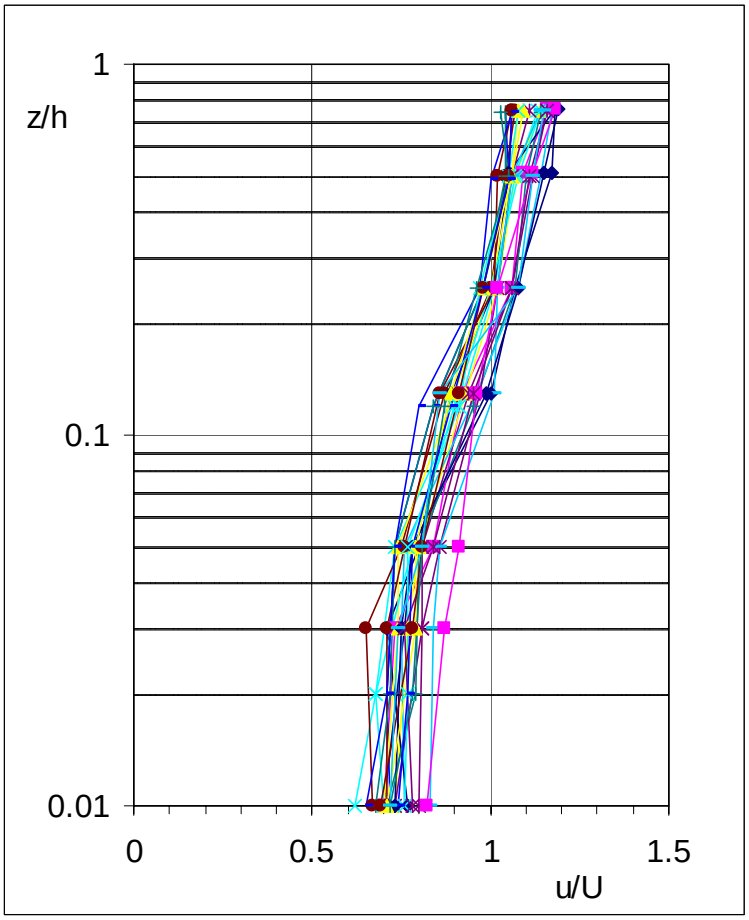

Figure 13. Profiles of measured velocity collected at all measurement stations for all flow conditions. Velocity is normalized by mean velocity.

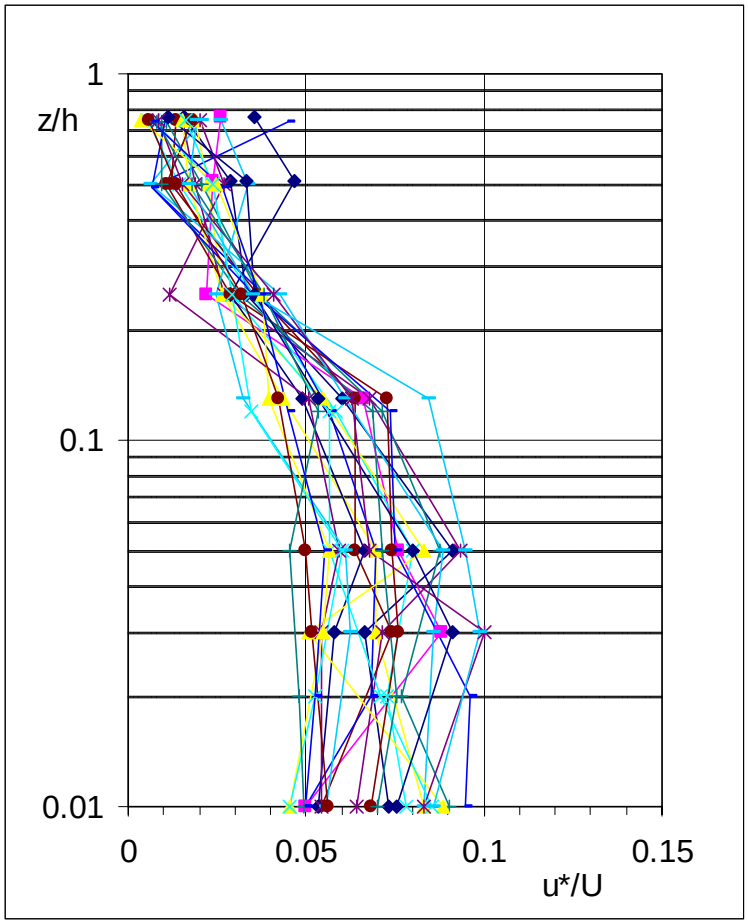

Figure 14. Profiles of shear velocity collected at all measurement stations for all flow conditions. Shear velocity is normalized by mean velocity.

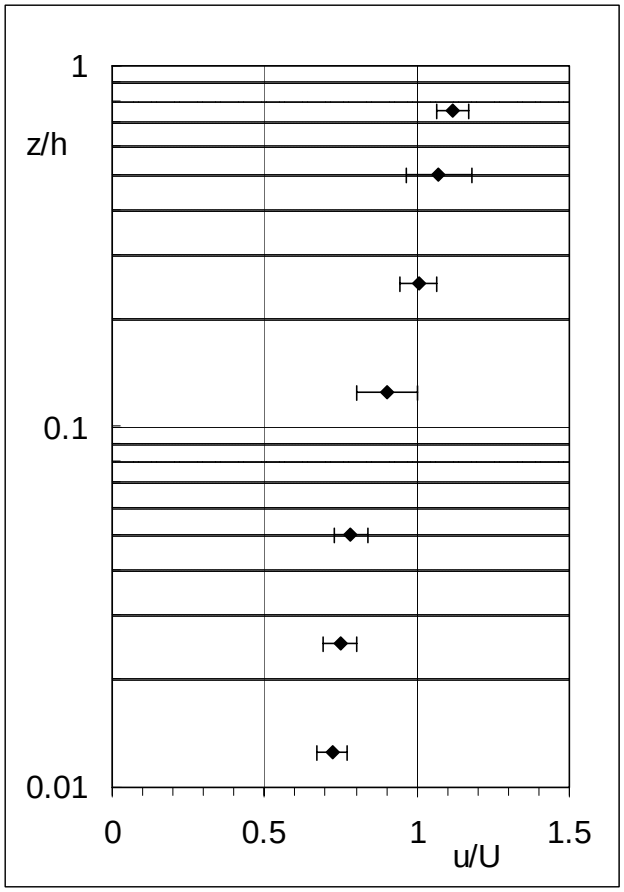

Figure 15. Velocity profile averaged among all flows and measurement stations.

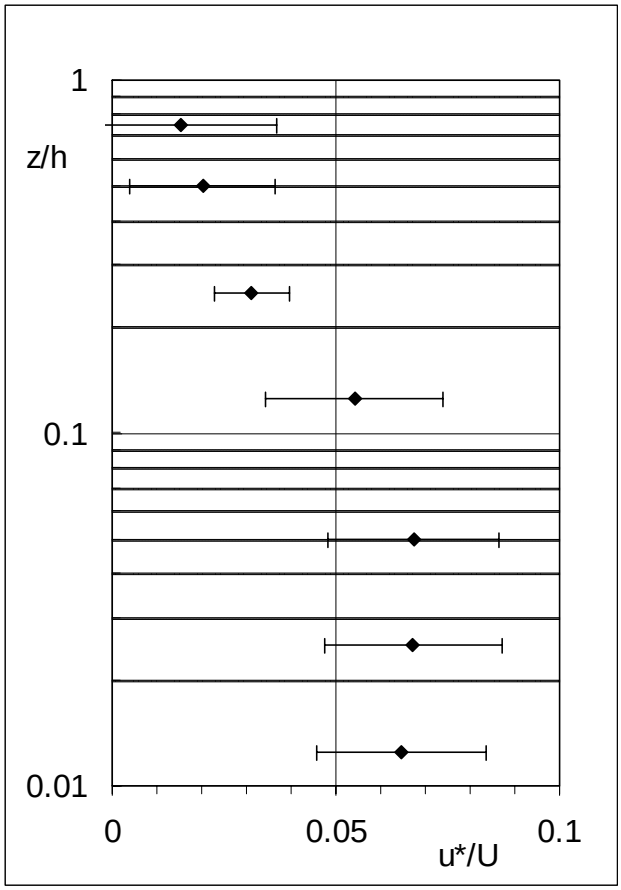

Figure 16. Profile of shear velocity, averaged among all flows and measurement stations.

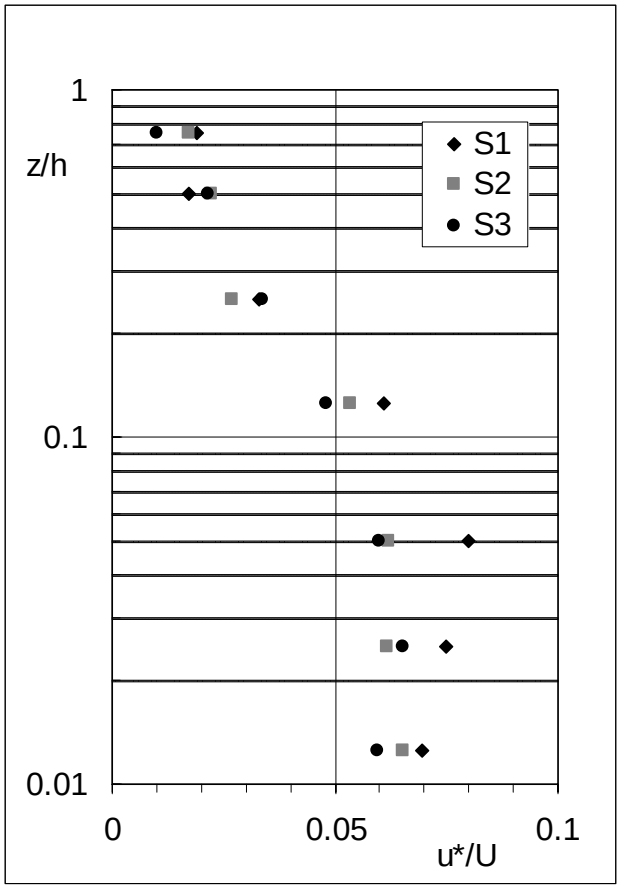

Figure 17. Shear velocity profile for each measurement station, averaged for all flow conditions.

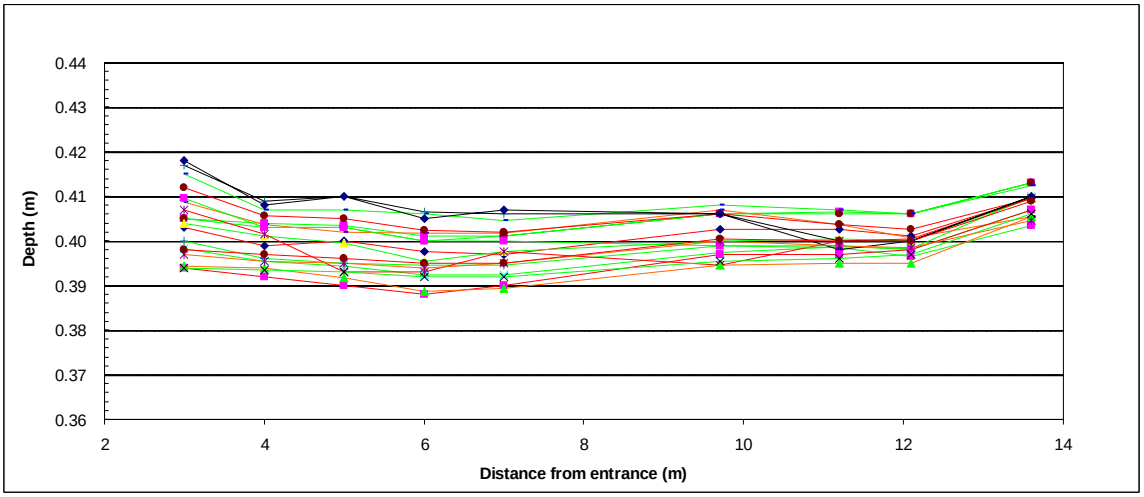

Figure 18. Profiles of flow depth for each of the flume runs showing non-uniformities at upstream and downstream ends.

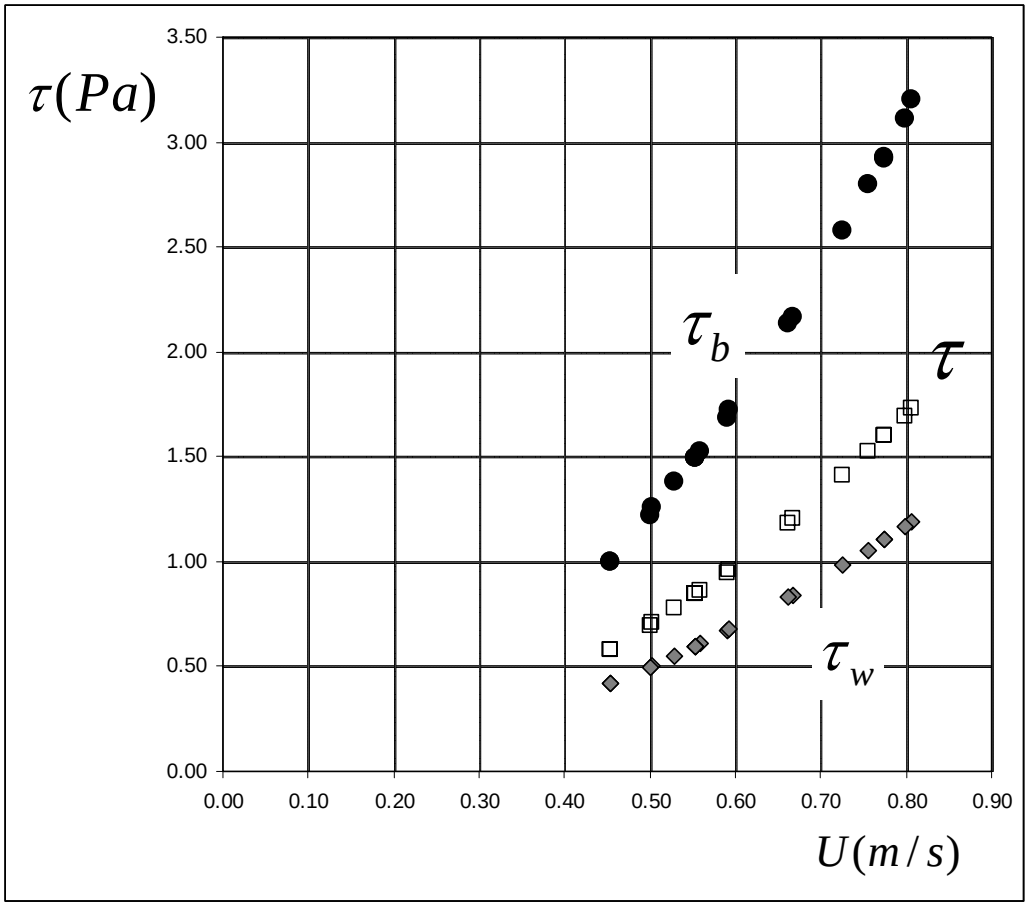

Figure 19. Bed stress τ_b as determined from near-bed Reynolds stresses plotted with wall stress τ_w and total stress τ as determined from sidewall correction procedure.

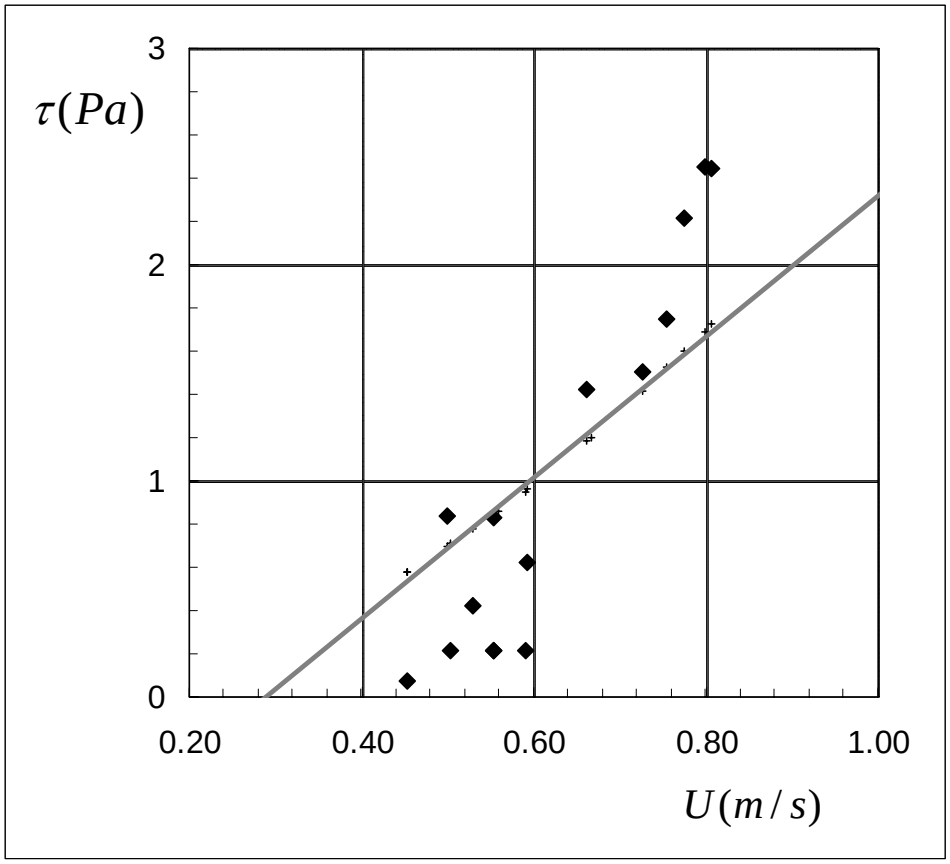

Figure 20. Total boundary shear stress as determined from non-uniform flow shallow water equation (diamonds) and the total stress based on the modeled u_*

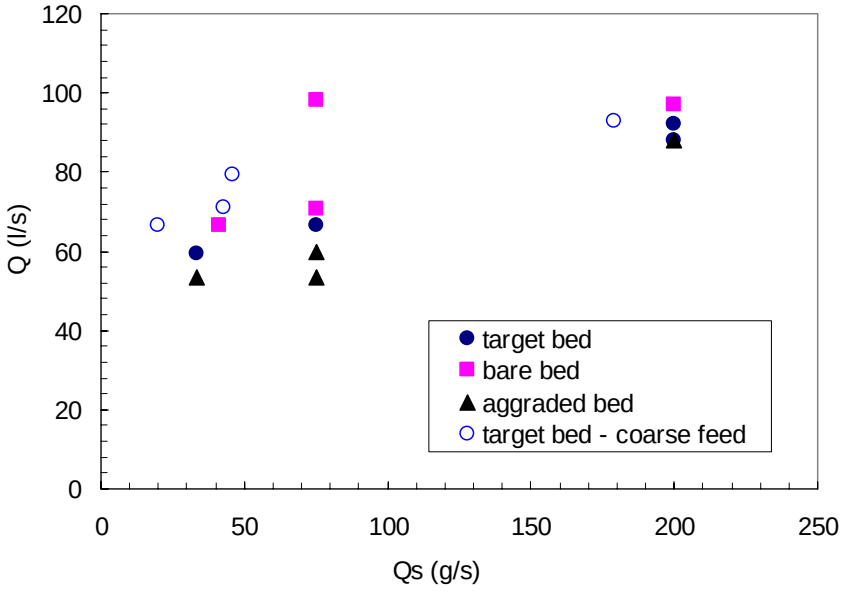

Figure 21. Plot of sediment feed rate (Q_s) and flow rate (Q) for uniform transport runs conducted in 2002.

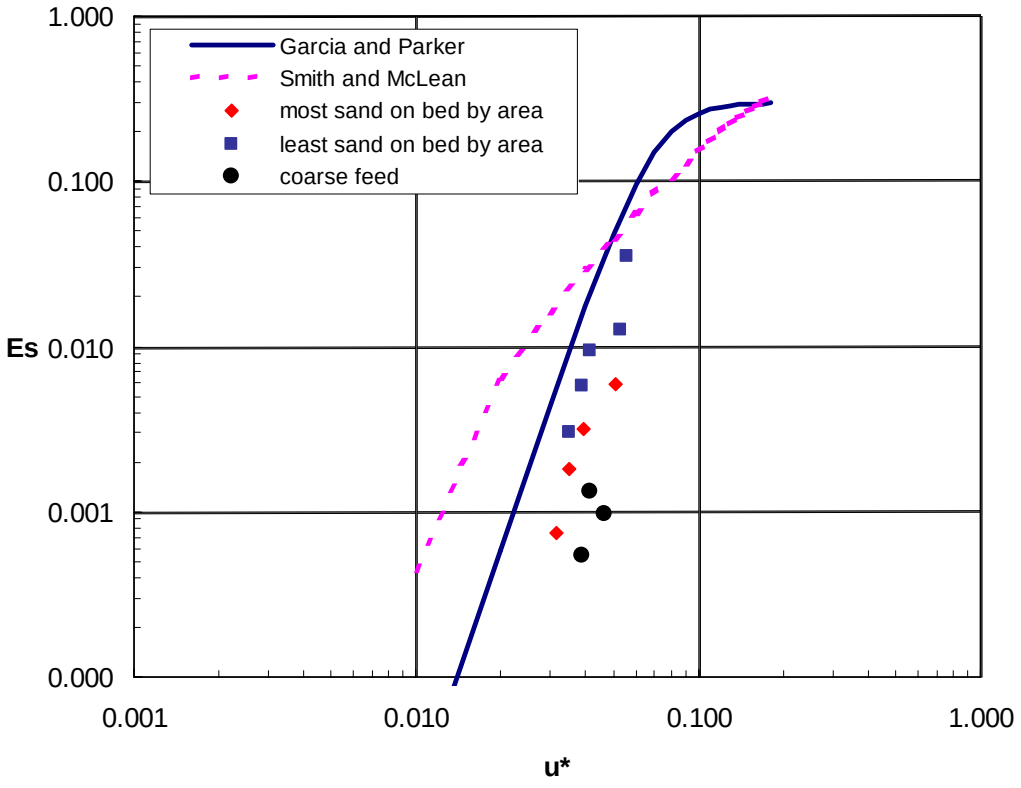

Figure 22. Observed near bed concentrations, plotted as entrainment rates, compared to the Garcia-Parker and Smith-McLean models. The dimensionless entrainment rate E_s is related to near bed concentration c_a as $E_s = \frac{c_a}{2.65 \times 10^6}$.

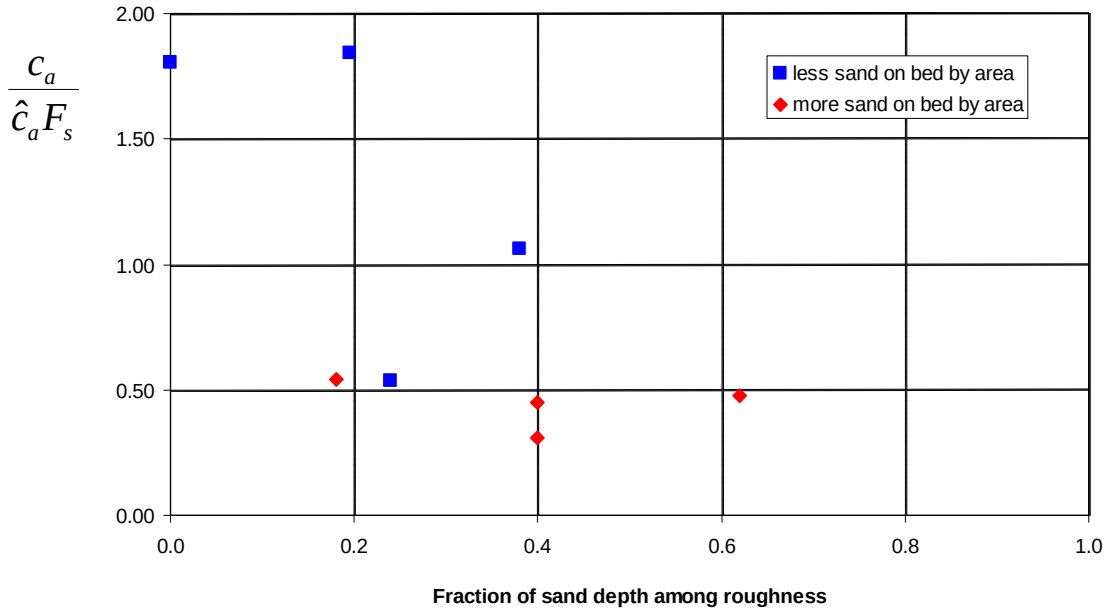

Figure 23. ϕ calculated as $c_a/\hat{c}_a F_s$ as a function of the fractional sand depth among the roughness.

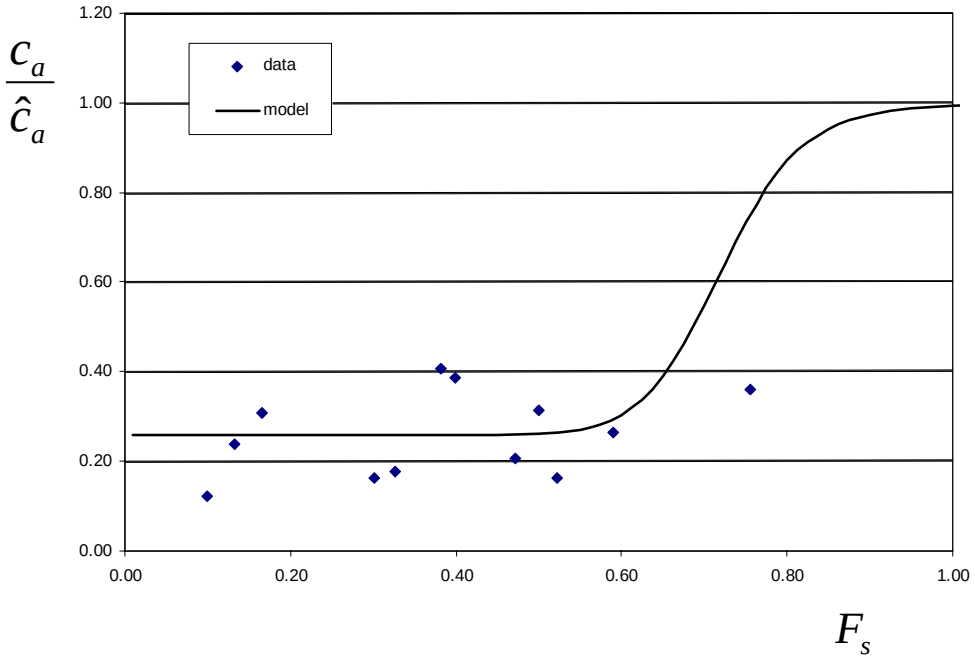

Figure 24. $F_s\phi$ calculated as $c_a/\hat{c}_a$ as a function of the fraction of the bed covered by sand.

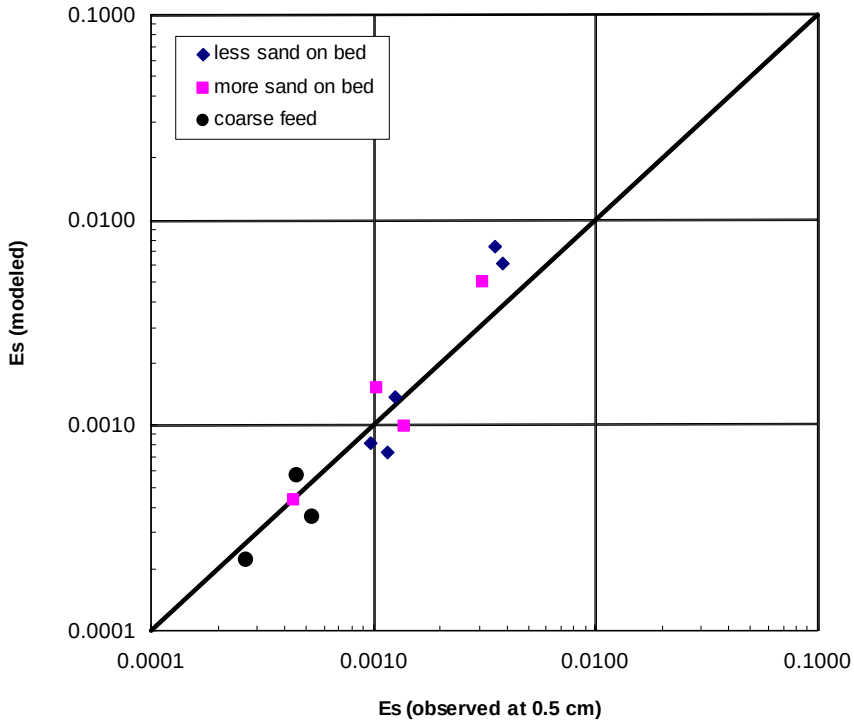

Figure 25. Modeled and observed near-bed concentrations for a height of 0.5 cm above the bed roughness elements.

Sand Routing Experiments Planned for April-June 2004

The results of the 2002 experiments (reported in 2003 progress report) have been used to formulate a working entrainment model that will be tested in sand routing experiments we will be conducting in the next few months. These experiments will include uniform and nonuniform transport conditions that will allow testing of the entrainment model by comparing observed bed behavior with that predicted by the coupled sand entrainment and routing model. The specific objective of these experiments is to produce a spatially uniform sand bed that partially buries the roughness elements, then introduce nonuniform transport conditions and track changes in bed elevation and grain size and suspended sediment concentration and grain size. These experiments are being conducted as an expansion of work described in our original proposal to the GCMRC and we have received supplemental funding from the National Center for Earth-surface Dynamics to partially cover facility and operations costs at Saint Anthony Falls Hydraulic Laboratory The complete proposal funded by SAFHL is in Appendix 2.

The flume used in the 2002 experiments was relatively small and a narrow width was used to achieve the needed flow depth. Sidewall effects influenced the flow field and caused accumulations of sand along the channel edges, making it difficult to clearly define the average bed elevation. The proposed second set of experiments will be conducted in a much larger facility (an 84 m long, 2.75 m wide, and 1.8 m deep channel

at the Saint Anthony Falls Laboratory) where it should be possible to minimize those secondary effects.

These experiments will use the same bed roughness as the initial experiments installed along a 50 m test section of the channel. Flow depth will be about 60 cm, only slightly greater than the initial experiments, to yield similar mean velocities and bed shear stresses. The primary feed sediment will have a median diameter of 0.12 mm, preserving the scaling properties described above for the 2002 runs. A preliminary run will be conducted to determine a discharge and sediment feed combination that will produce a spatially uniform bed below the roughness elements. Using the 2002 experiments as a guide, a mean velocity of about 50 cm/s with mean suspended sediment concentration of 600 mg/l should produce an acceptable "target" bed. In the large channel, this will require a discharge of approximately 812 l/s and sediment feed rate of about 1754 kg/hr. These will be used as trial conditions and adjusted to achieve a suitable bed. Once established, this discharge and sediment feed combination will be used as the standard for the four main experimental runs.

The experiments will each begin with 45 to 60 min period during which uniform transport conditions are established. Nonuniform transport conditions will then be introduced by either a change in sediment feed rate or sediment feed grain size. This perturbation is anticipated to cause a sediment wave, which will migrate downstream, as was observed in the initial experiments under nonuniform conditions. The experimental runs are proposed to be conducted as follows:

Run 1. *Uniform transport followed by evacuation*. Following the uniform transport period, sediment feed will be stopped. Measurements will track the lowering and coarsening of the sand bed.

Run 2. *Increase sand feed rate*. Following the uniform transport period, sediment feed will be increased by 25% for 15 min, and then returned to the standard rate. Measurements will track the migration of the added sediment.

Run 3. *Increase sand grain size*. Following the uniform transport period, sediment feed will be coarsened by adding 20% coarse sand (0.3 mm median diameter) to the feed mix for 15 min, then return to the standard feed. Measurements will track the migration of the coarse sand. Conclude run by eliminating feed and tracking the lowering and coarsening of the sand bed.

Run 4. *Increase sand feed rate and grain size*. Following the uniform transport period, sediment feed will be increased by 25% and coarsened as for Run 3 for 15 min, then return to standard conditions. Measurements will track the migration of the added coarse sand.

<u>Data that will be collected during and following runs:</u>

1) Following the test run the flow field for the standard discharge will be characterized using an ADV. Velocity profiles will consist of at least seven vertical sampling positions

and will be collected in a spatial array of at least 10 streamwise and 3-5 cross-stream sample locations. Measurements will be made for 1 min at a sampling rate of 25 Hz.

2) Suspended sediment samples will be collected using isokinetic siphons situated in vertical rakes with intake tubes positioned at five elevations above the bed. Three sampler rakes will be positioned along sections 30 m and 45 m below the upstream end of the test section. Samples will be collected at 15-20 min intervals throughout each run. This sampling arrangement may be adjusted depending on the availability of alternative sediment sampling instruments, such as acoustic sensors or LISST.

3) Bed elevation will be tracked continuously with acoustic sensors roughly 1m upstream of each suspended sampler array.

4) Colored sand will be substituted as the feed sand for 1 min at the end of the uniform transport period for each run. This will establish a marker bed facilitating distinction between the uniform transport bed and the nonuniform transport bed.

Model testing and evaluation

The data collected in the nonuniform flume experiments will be used to test the routing model, coupled with the entrainment model. Because these experiments will include bed segments with sand below the roughness tops and segments with migrating sand waves burying the bed roughness, it will be necessary to integrate the coarse-bed entrainment model with an existing model for sand transport over bedforms (e.g. Smith and Mclean, 1977; Mclean et al., 1999). Boundary and initial conditions, such as flow and sediment feed rate will be specified for each experimental run. The morphodynamic model can then be verified against measured bed topography. In order to implement the model, it will be necessary to discretize the system in time and distance down the channel. The appropriate time step will be related to the speed of movement of the suspended sediment and the bed sediment, and the distance step will be related to the length scale of the sediment waves.

The routing model will be evaluated by comparison of predicted bed behavior with observed bed behavior during the nonuniform transport experiments. As described above, it is expected that the introduced nonuniformity (i.e. increased feed rate or grain size) will produce a sediment wave that will migrate downstream. Upon resumption of standard sediment feed conditions, it is expected that the sand wave will continue to migrate downstream as the bed returns to uniform transport conditions. For the routing model to be successful, it should (1) reproduce the observed processes, which are expected to be sand wave deflation and migration, (2) represent these processes at the appropriate length and time scales, and (3) recover to uniform conditions following the perturbation.

References

Chiew, Y., and Parker, G., 1994, Incipient sediment motion on non-horizontal slopes: Journal of Hydraulic Research, v. 32, no. 5, p. 649-660.

Goring, D. G., and Nikora, V. I., 2002, Despiking acoustic doppler velocimeter data: Journal of Hydraulic Engineering, v. 128, no. 1, p. 117-126.

McLean, S. R., Wolfe, S. R., and Nelson, J. M., 1999, Predicting boundary shear stress and sediment transport over bed forms: Journal of Hydraulic Engineering-Asce, v. 125, no. 7, p. 725-736.

Nelson, J. M., Emmett, W. W., and Smith, J. D., 1991, Flow and sediment transport in rough channels, *in* Fifth Federal Interagency Sedimentation Conference, Las Vegas, Nevada.

Nelson, J. M., Shreve, R. L., McLean, S. R., and Drake, T. G., 1995, Role of near-bed turbulence structure in bed load transport and bed form mechanics: Water Resources Research, v. 31, no. 8, p. 2071-2086.

Smith, D. J., and McLean, S. R., 1977, Spatially averaged flow over a wavy surface: journal of geophysical research, v. 82, no. 12, p. 1735-17

Topping, D.J., D.M. Rubin, J.M. Nelson, P.J. Kinzel, and J.P. Bennett., 1999, Linkage between grain-size evolution and sand depletion during the Colorado River floods, in Webb, R.H., Schmidt, J.C., Marzolf, G.R., and Valdez, R.A. (eds.), The Controlled Flood in Grand Canyon: Washington, D.C., American Geophysical Union, Geophysical Monograph 110.

Vanoni, V. A., 1975, Sedimentation Engineering, American Society of Civil Engineers.

Wahl, T. L., 2000, Analyzing ADV Data Using WinADV, *in* Joint Conference on Water Resources Engineering and Water Resources Planning and Management, Minneapolis, Minnesota.

Wahl, T. L., 2003, Discussion of "Despiking acoustic doppler velocimeter data": Journal of Hydraulic Engineering, v. 129, no. 6.

Wiberg, P. L., and Smith, J. D., 1991, Velocity distribution and bed roughness in high-gradient streams: Water Resources Research, v. 27, no. 5, p. 825-838.

Wiele, S.M. and M. Torizzo, 2003, A stage-normalized function for the synthesis of stage-discharge relations for the Colorado River in Grand Canyon, Arizona: U.S. Geological Survey Water-Resources Investigations Report 03-4037, 23 p.

\

Appendix 1: Project-related presentation over the past year

Grams, P. and P. Wilcock, Canyon in a Box: Flume Studies of Sand Transport in Grand Canyon and Implications Modeling and Management, U.S. Geological Survey Southwest Biological Science Center Grand Canyon Monitoring and Research Center Colorado River Science Symposium October 28 – 30, 2003, Tucson, Arizona.

*Korman, J., S.M. Wiele, and M. Torizzo, Modeling Effects of Discharge on Habitat Quality and Dispersal of Juvenile Humpback Chub (*Gila cypha*) in the Colorado River, Grand Canyon, U.S. Geological Survey Southwest Biological Science Center Grand Canyon Monitoring and Research Center Colorado River Science Symposium October 28 – 30, 2003, Tucson, Arizona.

Wiele, S.M. and J. Hazel, Efficient use of water and sand in the maintenance of sandbars in the Colorado River below Glen Canyon Dam, Arizona Hydrological Society 2003 Annual Symposium, Mesa, Arizona, September 17-20, 2003.

Wiele, S.M., 2-Dimensional flow modeling, presented to the Technical Work Group, September, 2003, Phoenix, Arizona.

Wiele, S.M. and J. Hazel, Results from Modeling of Sand Deposition as a Function of Discharge and Sandbar Surveys: How Effective are Powerplant Flows at Making New Sand Deposits? U.S. Geological Survey Southwest Biological Science Center Grand Canyon Monitoring and Research Center Colorado River Science Symposium October 28 – 30, 2003, Tucson, Arizona.

*Wiele, S.M. and Torizzo, M., Modeling of Sand Deposition in Archaeologically Significant Reaches of the Colorado River in Grand Canyon, U.S. Geological Survey Southwest Biological Science Center Grand Canyon Monitoring and Research Center Colorado River Science Symposium October 28 – 30, 2003, Tucson, Arizona.

*Wiele, S.M., Flow and sediment transport modeling in the Colorado River in Grand Canyon, Lower Colorado River Science Workshop June 17 - 18, 2003, Parker, Arizona.

* These presentations featured results from flow and sediment transport modeling, but were funded by the GCMRC entirely or in part on earlier projects.

Appendix 2: Proposal to test near-bed sand concentration algorithm at SAFHL
Research Project Title: Sand routing over a coarse immobile streambed

Principal Investigator Information:

Peter R. Wilcock
Professor
Department of Geography and Environmental Engineering
Johns Hopkins University
3400 N. Charles St., Baltimore MD 21218
Phone: (410) 516-5421
Fax: (410) 516-8996
E-Mail: wilcock@jhu.edu

Key Personnel Information:

Paul E. Grams
Graduate Student
Department of Geography and Environmental Engineering
Johns Hopkins University
3400 N. Charles St., Baltimore MD 21218
Phone: (410) 516-5137
Fax: (410) 516-8996
E-Mail: grams@jhu.edu

Desired Start Date of Project : 06/01/03 (flexible; could start later)

Estimated Duration of Project (in months): three

NCED Research Area

1. **Focus Area 4: Integration of morphodynamic processes across environments and scales**
2. **Focus Area 1: Landscape and seascapes**
3. **Focus Area 2: Basin evolution**

The project investigates sand transport over a river bed of coarse sediment, a basic process of landscapes (Focus Area 1). It is designed to inform models of sand routing over reach to river scales (Focus Area 4). Sand routing through at the river scale is needed to model basin evolution (Focus Area 2).

Estimated Budget: *$24,978.28*

Proposal Abstract

Routing sediment through river channels of geomorphically significant length remains a difficult and unsolved problem in earth system dynamics. Unknown boundary conditions and unbounded error accumulation prohibit extensive application of detailed models, motivating a reach-averaged approach incorporating sediment source/sink terms that account for local sediment storage. The work proposed here contributes to a project in which we are developing a sediment routing model for 112 miles of the Colorado River below Glen Canyon Dam. The primary data available to test the model are accurate, but sparse: observations of sediment flux entering and leaving the modeling reach. Model development depends crucially on independent tests of individual components of the larger routing model. The components tested in the work proposed here are the near-bed sand concentration and sand bed elevation and grain size within a spatially nonuniform transport field.

Much of the bed in the Colorado River in the Grand Canyon is composed of large cobble and boulder. Nearly all of the transported sediment is fine to medium sand. Although theoretical formulations exist to extract form drag and predict near-bed suspension transport (e.g. Garcia and Parker, 1991; Nelson et al., 1991; Wiele and Franseen, 1999), there has been essentially no direct measurement of sand transport over large roughness elements. Recognizing this problem, our contract for the Grand Canyon sand routing model included lab experiments to provide measurements of suspended sand transport over large roughness elements. We completed these experiments in the tilting bed flume at SAFL in Summer 2002. We covered a 30cm wide bed with 10 cm hemispheres and measured transport of 0.12mm and 0.3mm sand for a range of water and sediment supply. These data are being used to test and revise a rough-bed suspension transport model.

While conducting experiments last summer, we hatched the plan for the work proposed here: a controlled, large scale test of the near-bed flow and transport model under nonuniform transport conditions. We will conduct four multi-part runs in a 50-m test section in the main SAFL channel. The new experiments provide test data for two coupled pieces of a sand routing model. Nonuniform transport in the main channel will provide a rigorous test of the near-bed flow/transport model, as well the sand routing algorithm. A problem of particular interest is prediction of transport under diminishing sand supply. As the sand bed deflates, the transport rate will depend on the increasing grain size of the sand bed (Topping et al., 2000) as well as the lowered sand bed relative to the top of the roughness elements. The balance between these two mechanisms plays a central role in determining both transport rates and available sand storage in a coarse-bedded river.

The transport in many coarse-bedded rivers consists primarily of fine-grained sediment. The data and the corresponding model of flow, sand transport, and bed evolution, have application well beyond the Colorado River in the Grand Canyon. Spatial nonuniformity in sediment transport over large roughness elements is a key element of an appropriate data set, but requires a very large flume. The SAFL main channel is one of the few in the world of sufficient size. The work proposed here is an expansion of an existing project and will provide information of importance to models for routing fine sediment through river networks. We will request salary support for this work from the original project

sponsor (Grand Canyon Monitoring and Research Center through the USGS) and request from NCED support for materials, labor, and a small amount of travel costs.

Research Objectives

(1) Develop both uniform and nonuniform transport of fine to medium sand over a bed of large roughness elements. Nonuniform transport fields will be produced by increasing the sediment feed rate, coarsening the sediment feed, and by a combination of the two. The migration of the sediment feed perturbation will be tracked. Winnowing of the bed under zero sediment feed will also be tracked.

(2) How does sand transport rate vary with changes in sand bed elevation and grain size? Does coarsening the sand bed reduce the transport rate as predicted by standard sand entrainment models? Does lowering the sand bed relative to the roughness elements reduce the sand entrainment, or are the wakes shed by the coarse elements sufficiently strong to entrain any sediment within the pores?

(3) Test existing models for near-bed drag partitioning, multi-size sand entrainment, and sand mass conservation for transport over large roughness elements.

Research Implementation Plan

A bed of 10cm (or 4 inch) diameter hemispheres will be placed in a 50m test section of the main channel. We propose an experimental design consisting of one preliminary run followed by an experimental matrix of four runs. The preliminary run will be used to establish a combination of discharge and sediment feed rate that produces a spatially uniform sand bed that partially buries the hemispheres. Based on the 2002 experiments, we find that a suitable bed forms within tightly constrained combinations of water and sediment feed. Trial discharge will be 620 l/s (depth 0.5m; mean velocity 0.56m/s) with a sand feed rate of about 2680 kg/hr. A flow and feed combination that produces a spatially uniform sand bed that partially buries the hemispheres defines the "standard" flow and feed rates for subsequent runs. We will explore bed and transport response to changes in the rate and grain size of sediment feed, using the same flow rate in all runs. Following the test run, we will chacterize the flow field at the standard discharge with a SAFL acoustic doppler velocimeter. The four run experimental matrix is designed to allow observation of both uniform and nonuniform transport fields, including migration of sediment feed perturbations and gradual evacuation of sand from the flume. The primary sand used is US Silica "F110" sand (D_{50}=0.12mm). In two runs, we supplement the F110 with a coarser sand ("Lakeland"; D_{50}=0.3mm) in order to investigate sediment sorting effects. Colored F110 sand will also be used for short intervals in each run to establish marker beds and evaluate mixing depth within the sand beds.

Run 1 (uniform transport with evacuation): Establish uniform bed at std. flow and sediment feed (60 min), then eliminate sediment feed and track lowering and coarsening of the sand bed (20 min segments). Switch to colored sand for one minute at 59 min. Flume drained and bed sampled at 60 min and following each winnowing segment.

Run 2 (increase rate of sand feed): Establish uniform bed at std. flow and sediment feed (45 min), increase sediment feed rate by 25% (15 min.), then return to standard conditions to track the migration of the added sediment through the system (60 min). Switch to colored sand for one minute at 44 min. Flume drained and bed sampled at 60 min, 80 min, 100 min, and 120 min.

Run 3 (increase rate and grain size of sand feed): Establish uniform bed at std. flow and sediment feed (45 min), increase feed rate by 25% using Lakeland sand for the supplemental feed (15 min.), then return to standard conditions to track the migration of the added sediment through the system (60 min). Switch to colored sand for one minute at 44 min. Flume drained and bed sampled at 60 min, 80 min, 100 min, and 120 min.

Run 4 (increase grain size of sand feed): Establish uniform bed at std. flow and sediment feed (45 min), change to sediment supply at same rate but with 20% Lakeland for 15 min., then return to standard conditions to track propagation of coarse sand (60 min). Follow with zero sediment feed to track lowering and coarsening of the sand bed (20 min segments). Switch to colored sand for one minute at 44 min. Flume drained and bed sampled at 60 min, 80 min, 100 min, 120 min, 140 min, 160 min., 180 min.

Data Collection

Standard observations during runs: (a) point sediment concentrations using isokinetic siphons situated in vertical rakes of five tubes. Three sampler rakes will be positioned along sections 30m and 45m downstream of the upstream end of the test section. (b) bed elevation tracked with acoustic sensors roughly 1m upstream of each suspended sampler array. Following each run segment, the sand bed thickness and configuration will be mapped and spot sampled for stratigraphy and grain size.

Required Research Facilities & Materials

1) Main SAFL channel. A bed of 10cm diameter hemispheres will be installed in a 50m test section. Each row of hemispheres is offset 1/2 diameter; alongstream row spacing will be 10cm (i.e. not closest packing) to provide storage space for a sand bed. Approximately 13,500 hemispheres are needed, so a mass-produced source is needed (masonry provides ease of installation, but high transport and disposal costs; plastic or foam may be inexpensive (Slurpee lids?), but require adhesives). Preservation of the bed during flow shut-down requires ability to rapidly stop the flow and slowly drain the flume. A weighted plywood sheet may provide a suitably rapid and leaky drop gate

2) Sediment feed. Based on our 2002 experience, we expect that a 4-person sediment feed crew can maintain a consistent sediment feed at the desired rates (~ 2680 kg/hr for up to two hours and ~ 3350 kg/hr for up to 15 minutes). Automated feed would be desirable but is likely to be prohibitively expensive. Staging for 6 tons of sand needed at upstream end of main channel.

3) Sediment: We estimate using about 22 tons of US Silica F110 and 2 tons of the Lakeland sand.

4) Sediment lab (oven, balance) for processing suspended sediment samples.

Required Instrumentation

1) ADV for characterizing flow (needed for ~ 1 week, not needed for experimental runs)
2) Sediment sampling – Six 'rakes' of five siphon tubes each, with tubing to deliver samples to collection point outside of flume.
3) Bed elevation sensors – continuous tracking of bed elevation at six locations. Acoustic sensors are the likely solution.

Project Schedule and Timeline

Week	Task
1-4	Preparation of sediment bed; sediment feed facility
5-6	Instrumentation development (sediment samplers and bed elevation)
7	Preliminary runs to establish standard discharge and sediment feed rate.
8	Flow runs (ADV profiles; set up and calibrate suspended sediment siphons)
9	Run 1. uniform transport with evacuation
10	Run 2. increase rate of sand feed
11	Run 3. increase rate and grain size of sand feed
12	Run 4. increase grain size of sand feed

Personnel

Paul Grams will be on site for the entire 3 month work period. Peter Wilcock will work at SAFL during weeks 7, 9, 10, and 11.

References

Garcia, M., and G. Parker. 1991. Entrainment of bed sediment into suspension. Journal of Hydraulic Engineering **117**:414-435.

Nelson, J. M., W. W. Emmett, and J. D. Smith. 1991. Flow and sediment transport in rough channels. *in* Fifth Federal Interagency Sedimentation Conference. Interagency Advisory Committee on Water Data, Subcommittee on sedimentation, Las Vegas, Nevada.

Topping, D. J., D. M. Rubin, J. M. Nelson, P. J. I. Kinzell, and I. C. Corson. 2000. Colorado River sediment transport 2. Systematic bed-elevation and grain-size effects of sand supply limitation. Water Resources Research **36**:543-570.

Wiele, S. M., and M. A. Franseen. 1999. Use of reach-averaged properties and characteristic environments in the routing of sand in a river of complex morphology. EOS, Transactions American Geophysical Union, Annual Meeting, Spring 1999.

Estimated Budget:

Project Title:

Sand routing over a coarse immobile streambed

NCED Reseach Staff Salaries	**Rate/day****	**Days**	**Cost**
Machinist (M. Plante)	$ 287.04	2.5	$ 717.60
Instrumentation Specialist (C. Ellis)	$ 374.88	5	$ 1,874.40
Junior Scientist	$ 207.44	0	$ -
Junior Scientist Trainee	$ 80.00	60	$ 4,800.00
	Sub-Total Salary		**$ 7,392.00**
Materials and Supplies			**Cost**
Sand (22 tons F110; 0.5 ton Lakeland)			$ 3,000.00
Bed materials (13,500 hemispheres; substrate material or adhesive)			$ 4,000.00
Tubing for sediment siphon sampler			$ 500.00
<Enter material or supply cost here>			$ -
<Enter material or supply cost here>			$ -
	Sub-Total Materials and Supplies		**$ 7,500.00**
Travel (Example: airfare, taxi, car rental)			**Cost**
2 roudntrip discount airfares (Balto-MSP)			$ 500.00
			$ -
			$ -
	Sub-Total Travel		**$ 500.00**
Per-Diem (Example: housing, meals)	**Rate/day**	**Days**	**Cost**
Wilcock housing (4 weeks @$200)	$ 100.00	8	$ 800.00
Grams housing: no cost	$ 100.00	**$ 24,978.28**	$ -
No meals requested	$ 100.00	0	$ -
	Sub-Total Per-Diem		**$ 800.00**
TOTAL DIRECT COST			**$ 16,192.00**
INDIRECT COST (59% of I and II)			**$ 8,786.28**
GRAND TOTAL			